Temperature and field dependence of the intrinsic tunnelling structure in overdoped $Bi_2Sr_2CaCu_2O_{8+\delta}$

T. M. Benseman,[1,*] J. R. Cooper,[1] and G. Balakrishnan[2]

[1]*Physics Department, Cavendish Laboratory, University of Cambridge, J.J. Thomson Avenue, CB3 0HE, United Kingdom*
[2]*Department of Physics, University of Warwick, CV4 7AL, United Kingdom*

We report intrinsic tunneling data for mesa structures fabricated on three over- and optimally-doped $Bi_{2.15}Sr_{1.85}CaCu_2O_{8+\delta}$ crystals with transition temperatures of 86–78 K and 0.16–0.19 holes per CuO_2 unit, for a wide range of temperature (T) and applied magnetic field (H), primarily focusing on one overdoped crystal (OD80). The differential conductance above the gap edge shows a clear dip structure which is highly suggestive of strong coupling to a narrow boson mode. Data below the gap edge suggest that tunnelling is weaker near the nodes of the d-wave gap and give clear evidence for strong T-dependent pair breaking. These findings could help theorists make a detailed Eliashberg analysis and thereby contribute towards understanding the pairing mechanism. We show that for our OD80 crystal the gap above T_c, although large, is reasonably consistent with the theory of superconducting fluctuations.

I. INTRODUCTION

Despite intensive and wide-ranging research in the past thirty years, detailed understanding of the fundamental physical properties of high temperature cuprate superconductors, especially the pairing mechanism, remains elusive. Much of the microscopic information about their fascinating electronic properties comes from surface probes such as angle-resolved photoemission (ARPES) [1] and scanning tunneling microscopy (STM) [2–4], while in the past decade measurements of transport, e.g., Ref. [5] and structural properties, e.g., Refs. [6,7] in extremely high magnetic fields have also been fruitful. It is important to verify the results of the surface probes by bulk measurements whenever possible. For many years it has been known that mesa structures fabricated from highly anisotropic high-T_c superconductors such as $Bi_2Sr_2CaCu_2O_{8+\delta}$ (Bi-2212) may be regarded as stacks of planar "intrinsic tunnel junctions" (ITJs) connected in series, and their I-V characteristics correspond to c-axis, superconductor-insulator-superconductor (SIS) tunneling spectra [8]. Planar geometry was used for the groundbreaking tunneling work on classical superconductors [9] and tunneling in planar ITJs may be easier to understand than in break junctions [10–12] where different junctions may sample different regions in **k** space. Furthermore one of us has argued [13] that in STM studies the tunneling probability may have significant **k** dependence. A longer term goal of the present work is to understand the structure we observe above the gap edge and see whether it can be analyzed using Eliashberg theory [14,15] to give direct information about a pairing boson. It will also be important to compare any such results with Eliashberg analysis of the optical reflectivity [15] which can be performed over a much wider energy range. In the present paper we do not attempt this but report high quality ITJ data and highlight some unexpected findings regarding the temperature (T), voltage (V), and magnetic field (H) dependence of the tunneling characteristics observed.

In an earlier report [16] we showed experimental data for ITJs fabricated on two overdoped single crystals of Bi-2212 with T_c values of 80 and 78 K, denoted OD80 and OD78, and an optimally doped crystal, OP86 with $T_c = 86$ K. Tunnelling results for the latter crystal and others with hole concentrations $p < 0.19$ per CuO_2 unit are probably complicated by the presence of the pseudogap and also of charge density waves that have been observed for both Bi-2212 [3,4] and $YBa_2Cu_3O_{6+x}$ (YBCO) with x between 0.45 and 0.93 [17]. Here we focus more on OD80, so our data are complementary to a recent ITJ study [18] dealing with moderately and slightly underdoped Bi-2212 crystals that do have a pseudogap. Our interpretation is different in that we suggest that in OD80 the clear T-dependent structure above $2\Delta_0$, where $\Delta_0(T)$ is the superconducting gap at the antinodes, could arise from coupling with pairing boson(s) and not from the pseudogap. For such overdoped crystals ARPES [1] and STM [3] data gives evidence for a large Fermi surface and no pseudogap at low T, which is in agreement with bulk probes such as specific heat [19], static magnetic susceptibility [19,20], and measurements of the London penetration depth [21,22]. In our tunneling data for OD80 there is evidence for a gap persisting above T_c. We argue that it is consistent with the microscopic theory [23] of superconducting fluctuations based on the Ginzburg-Landau free energy expansion, with relatively small values of the Ginzburg temperature, τ_G.

II. METHODS

Single crystals of Bi-2212 were grown using a traveling solvent floating zone furnace and feed rods with nominal stoichiometry of $Bi_{2.15}Sr_{1.85}CaCu_2O_{8+\delta}$. These have a maximum T_c of 86.5 K measured by SQUID magnetometry before

*Present address: Department of Physics, Queens College of the City University of New York, 65-30 Kissena Blvd., Queens, New York 11367, USA.
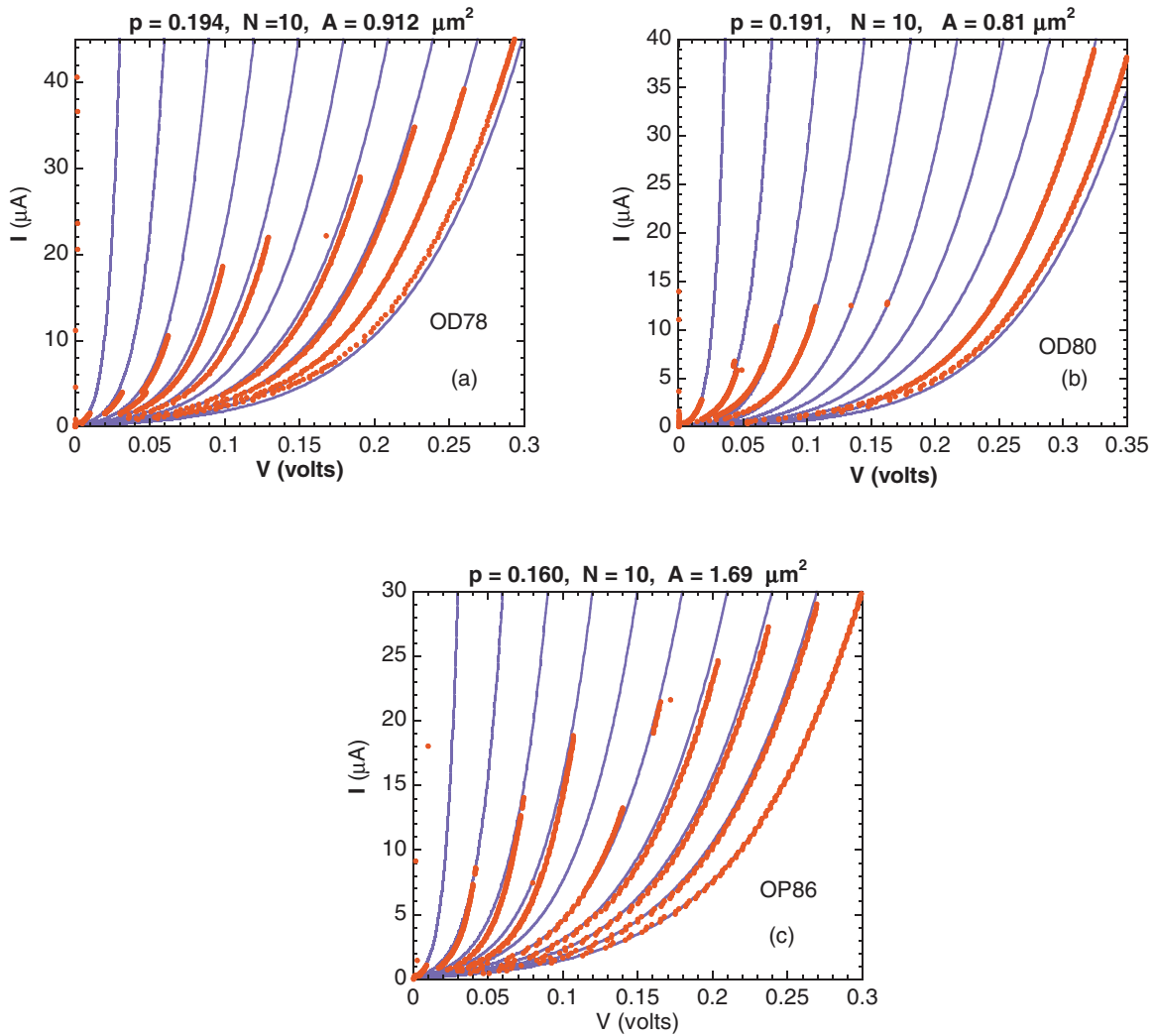
FIG. 1. Typical I-V curves for the three mesas at low bias voltages. Red points show data taken at 10 K while increasing I to an appropriate maximum value and then decreasing it. This generates a series of curves in which, from left to right, the Josephson currents of an increasing number of junctions are suppressed because there is a finite voltage across them. The blue lines show fits of the form $I = m_1 V + m_2 V^3 + m_3 V^5$ to the $(N-1)$th curve. The coefficients m_1, m_2, and m_3 are then scaled by $[(N-1)/n]^i$ where $i = 1, 3$, and 5, respectively, and n is an integer between 1 and N. Differences between the red data points and the blue lines give an indication of possible nonuniformity in junction areas, or more likely, their resistances.

fabrication of the mesas, and we infer p from the empirical relation [24] $T_c = T_c^{\max}(1 - 82.6[p - 0.16]^2)$, finding $p = 0.194$, 0.191, and 0.16 for the three crystals studied. For OD80, T_c measured by SQUID magnetometry agrees to within 1 K with the temperature where $2\Delta_0(T)$, defined by the maxima in dI/dV curves and shown in Fig. 6(b), reaches its minimum value of 34 meV. For OD78 and OP86, the minima in $2\Delta_0(T)$ are 2 K and 6 K lower than T_c values from SQUID magnetometry. The 6 K discrepancy for OP86 is probably caused by the presence of the pseudogap. This is not a problem because in Fig. 2(a) the values of dI/dV at high V show that the doping level of mesa OP86 is significantly less than that of OD80, while that of OD78 is slightly larger, in qualitative agreement with p values obtained from SQUID magnetometry. Typical I-V characteristics for the three mesas at small bias, taken while sweeping the current up and down in a controlled manner at 10 K, are shown in Fig. 1. The branches correspond to different numbers of Josephson junctions being

switched into the resistive state. Switching to another branch occurs when the critical (Josephson) current of a particular junction is exceeded and a voltage develops across it. The computer-controlled current is then swept down to a finite value before being increased again. When I is large enough, all Josephson currents are suppressed, there are no further jumps in V, and the extreme right hand red curves, extending to the largest values of V, are obtained. The number of junctions (N) in the stack is equal to the total number of branches observed. As shown in Fig. 1, these branches scale on to each other to a large extent, confirming that the junctions in the mesa have uniform area, and therefore all junctions switched to the resistive state will have the same voltage bias. However variations in resistance at the level of 10–15% do have significant effects on the magnitude of the structure in dI/dV above the gap edge. This is a prime cause of a certain lack of reproducibility in this structure, e.g., between data for OD80 and OD78 in Ref. [16] and shown later in Fig. 2(a)
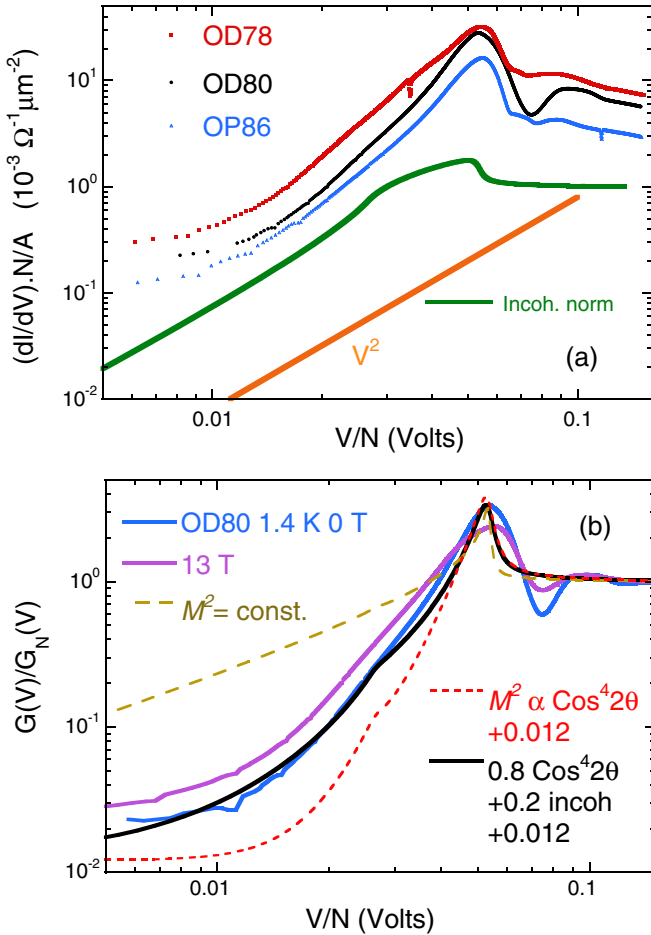
FIG. 2. (a) Log-log plots of dI/dV curves measured for the three mesas at 1.4 K in zero magnetic field when sweeping I down from its maximum value. The green curve agrees with an earlier calculation [25] and shows that purely incoherent tunneling gives completely different behavior. (b) dI/dV for mesa OD80 at 1.4 K in 0 and 13 T fields after normalizing to the normal state conductance. The solid black curve corresponds to a normalized coherent part calculated from Eqs. (1) and (2) with $M^2 \propto (\cos 2\theta)^4$, and multiplied by 0.8 plus a normalized incoherent part multiplied by 0.2. It gives a good description of the data below $V = \Delta_0$ after adding a small residual term, 0.012, to $G(V)/G_N(V)$. The longer and shorter dashed curves show the calculations for purely coherent tunneling with M^2 constant and $M^2 \propto (\cos 2\theta)^4$, respectively.

as well as for underdoped mesas [26]. Mesa dI/dV spectra [26] were measured as the bias current was swept down from its maximum value towards zero, thereby maintaining the resistive state. A lock-in technique with a small 77.7 Hz current modulation was employed, although standard I-V curves were recorded simultaneously.

The power dissipation per unit area in HTS mesa structures is large, sometimes resulting in extreme distortion of I-V curves by self-heating effects and consequent obliteration of any weak features in dI/dV. Zhu *et al.* [27] have studied mesa structures in near-optimally doped Bi-2212 containing $N = 10$–11 junctions in series, finding that there is little heating-induced distortion of the I-V characteristic only when the mesa area A is $\simeq 1$ μm^2 or less. Here all three mesas have

$N = 10$, the OD78 and OD80 mesas have A below this limit while OP86, although larger, has twice the resistivity above T_c. A high level of oxygen homogeneity in the mesa is necessary to ensure that any structure in dI/dV is observed. To avoid possible problems with ion milling [28], we fabricate our mesas solely by chemical wet etching [26]. Finally, irrespective of the size of the mesas, there is a possibility of electron heating. For a given V this will not depend on N or A but only on the electrical resistance of the junction per unit area and the thermal resistance for heat transfer between quasiparticles and phonons. We can rule this out for the OD80 mesa in Fig. 7 because the structure at higher V continues to evolve between 10 and 1.4 K.

III. BASIC THEORETICAL BACKGROUND

The origin of the pairing mechanism in cuprate superconductors continues to attract the attention of many talented condensed matter theorists. We hope that some of the points made here will contribute towards their understanding of this problem. Within the simple "semiconductor" picture for SIS tunneling [9] and writing the matrix element for tunneling from **k**-space angle θ_1 in electrode 1 to angle θ_2 in electrode 2 as $M_{\theta_1 \theta_2}$, the expression for the tunnel current between two identical electrodes is given by:

$$I(V) = \int_0^{2\pi} \int_0^{2\pi} \int_{-\infty}^{\infty} \left| M_{\theta_1 \theta_2} \right|^2 N(E, \theta_1) N(E - eV, \theta_2)$$
$$\times \left[f(E - eV) - f(E) \right] dE d\theta_1 d\theta_2, \quad (1)$$

where E is the energy of a Bogoliubov quasiparticle measured from the Fermi energy, $N(E, \theta)$ is the angle-dependent quasiparticle density of states (DOS) whose form in the Dynes approximation [29] is given in Eq. (2), and f is the Fermi function. As explained in Ref. [30] a distinction needs to be made between incoherent tunneling where the in-plane component of **k** is not conserved and coherent tunneling where it is approximately conserved, see Ref. [31]. For incoherent tunneling $|M|^2$ can be taken outside the integral and I is given by the product of two angular integrals of the density of states factors. For coherent tunneling $|M|^2 = |M(\theta_1)|^2 \delta(\theta_1 - \theta_2)$ and there is only one angular integral. Theoretically [30,32], $M(\theta)^2$ is expected to vary as $(\cos k_x - \cos k_y)^4$ or $(\cos 2\theta)^4$ in the notation used here.

As shown in Figs. 2(a) and 2(b) the dI/dV curve calculated for incoherent tunneling has a completely different shape to that for coherent tunneling and the latter is more similar to our experimental data. For completeness, in Fig. 2(b) we also show the case where $M(\theta)^2$ is constant to illustrate the contrast with incoherent tunneling shown in Fig. 2(a). It has been argued [30] that in the coherent case the antinodal states completely dominate the overall $G(V) \equiv dI/dV$ curves. We think this viewpoint needs further evaluation because it depends on the presence of a substantial antinodal Van Hove singularity deduced [30] from ARPES studies, which as pointed out by Loram [33] may not be not consistent with the weak T dependence of the paramagnetic susceptibility [19,20]. In later discussion, for simplicity, we consider a cylindrical Fermi surface for which there is no Van Hove singularity. Previous work on ITJs [34–36] also concluded that there was a certain amount of coherent tunneling, but only at the level [34] of 10%.

The theoretical curves in Fig. 2 were obtained using the Dynes formula [29] for $N(E,\theta)$ of a d-wave superconductor, namely:

$$N(E,\theta) = n(0,\theta)Re\left[\frac{|E| - i\Gamma}{\sqrt{(|E| - i\Gamma)^2 - (\Delta_0 \cos 2\theta)^2}}\right]. \quad (2)$$

Here Γ is the Dynes damping factor and $n(0,\theta)$ is the normal state DOS per unit energy per spin per radian at the Fermi energy. For an isotropic, cylindrical Fermi surface, $n(0,\theta) = n(0)/(2\pi)$, where $n(0)$ is the normal state DOS per unit energy per spin. The Dynes formula was originally used to extract the lifetimes (recombination rates) of excited quasiparticles in classical superconductors [29] from the T-dependent broadening of tunneling curves. It is somewhat different from the formula used to describe various pair-breaking effects in classical superconductors [37], for example by magnetic impurities. Namely the Dynes formula gives some zero-energy excitations for any nonzero value of Γ/Δ, while the pair-breaking formula only gives zero-energy excitations (referred to as gapless behavior) when the scattering rate exceeds a certain threshold value. The calculated curves in Figs. 2(a) and 2(b) correspond to an empirical formula, $\Gamma = 0.009 + 0.07x^4/(1 + x^2)$, where $x = E/\Delta_0$. We include the $x^4/(1 + x^2)$ factor because if Γ is independent of E then the curve calculated for the coherent case shows a strong anomaly at $V = \Delta_0$ that is not observed experimentally. This arises from the joint effect of the peak in the DOS at the antinode, $\theta = 0$, where $E = \Delta_0$ in electrode 1 and the residual DOS at $E = 0$, caused by there being nonzero Γ at the same angle in electrode 2. The formula used substantially reduces the anomaly at $V = \Delta_0$ but still does not account for the width of the peaks at $eV = 2\Delta_0$. It corresponds approximately to expectations for electron-electron scattering in a d-wave superconductor where the DOS varies as E for $E \lesssim \Delta_0$, has a weak logarithmic singularity at Δ_0 and becomes constant at higher E. In this case the usual E^2 behavior for electron-electron scattering with a constant (E independent) DOS changes over to E^4 at low E where there are two extra factors of E arising from the linear behavior of the DOS. However electron-electron scattering is not the only possible cause of an energy-dependent damping factor Γ: In a d-wave superconductor there are unoccupied quasiparticle states at arbitrarily low energies, so it could arise from inelastic scattering of quasiparticles by the pairing bosons.

As shown in Fig. 2(b), an angular independent coherent tunneling matrix element is ruled out and for the damping used we can fit our data with the sum of a dominant (80%) coherent term with $M^2 \propto (\cos 2\theta)^4$ and a smaller (20%) incoherent contribution. Equations (1) and (2) give a coherent contribution $G_S(0) = \int M(\theta)^2 [n(0,\theta)\Gamma(\theta)/\Delta(\theta)]^2 d\theta$ per spin channel for regions of the Fermi surface with $\Gamma(\theta) \lesssim \Delta(\theta)$, while quasiparticles in regions where $\Gamma(\theta) \gtrsim \Delta(\theta)$ will be essentially normal. For a d-wave superconductor with an angle-dependent gap $\Delta(\theta) = \Delta_0 \cos 2\theta$, such normal regions will have an angular spread of $\pm\Gamma/(2\Delta_0)$ radians around each node and contribute $\delta n(0) \equiv (2/\pi)\Gamma n(0)/\Delta_0$ to the DOS of an isotropic cylindrical Fermi surface. Usually their **k** states will be mixed by scattering and their tunnelling will be effectively incoherent, giving a contribution of $\langle M^2\rangle \delta n(0)^2$ to $G_S(0)$. Because $M^2 \propto (\cos 2\theta)^4$, $\langle M^2\rangle$, its average value near the nodes, will be small and as explained later, any contribution

to $G_S(0)$ from quasinormal regions near the nodes will be dominated by the 20% incoherent part shown up by the fit in Fig. 2(b).

The log-log plots in Fig. 2(a) show the overall reproducibility of $dI/dV \equiv G(V)$ curves rather directly in that the three curves are essentially parallel. A key point in any analysis is the reproducibility of the values of $G_S(0)$ when normalized to their values at high $V \simeq 0.15V$ or $5.5\Delta_0$, both for the 3 ITJs in Fig. 2(a) and for data in the literature [34,35]. Because of the reappearance of small Josephson currents at low V as I is swept down, we have obtained more precise values of $G_S(0)/G_N(0)$ from the $I(V)$ curves measured at the same time as dI/dV. This was done initially by fitting the data between 0.06 to 0.018 V, to $I = m_1(V/\Delta_0) + m_2(V/\Delta_0)^3 + m_3(V/\Delta_0)^5$ with $\Delta_0 = 0.027V$, but later it was found that straight-line fits to $I/V = m_1 + m_2(V/\Delta_0)^2$ showed up unwanted jumps from Josephson currents more clearly and gave less scatter in the values of m_1. In order to convert $G_S(0)$ into a residual DOS we also take into account the V dependence of the conductance $G_N(V)$ in the normal state using polynomials given in Ref. [38]. The H dependence of $G_S(0)/G_N(0)$ for the three mesas obtained from the latter m_1 values, i.e., straight line fits to plots of I/V vs V^2, is shown later in Fig. 4. It can be seen that all three mesas are consistent with $G_S(0)/G_N(0) = 0.012 \pm 0.001$ at $H = 0$. It is interesting to compare this with the normalized DOS $0.138/1.2 = 0.115 \pm 0.005$ obtained from the low T specific heat data for Bi-2212 in Ref. [39], where the specific heat coefficient $\gamma = 0.138$ mJ/gm-at./K^2, and the estimated normal state value $\gamma_n = 1.2$ mJ/gm-at./K^2 at low T given in Ref. [19]. This value is also consistent with microwave conductivity data on two optimally doped Bi-2212 crystals [40], which showed a residual normal fluid fraction of 0.11 and 0.12 for the simpler (Drude) analysis, or alternatively 0.15 and 0.16 for a non-Drude one, as well as with various heat capacity studies of YBCO [41–43]. However in response to a suggestion from one of the referees we have also fitted data for the lowest voltage branches of the I-V curves shown in Fig. 1 to $I/V = \alpha + \beta V^2$ and compared the coefficients α and β with m_1 and m_2 obtained on downward sweeps when all 10 junctions are resistive. Details for the three mesas are given as a table in the Supplemental Material [44], where it can be seen that m_1 and m_2 are systematically 20–40% larger than α and β. It is not clear at present whether this represents an interesting physical effect or whether it could arise from an unwanted extra conductance path (with a resistance of $\simeq 0.4$ MΩ) in parallel with the 10 junctions. In either case it implies that the residual conductances estimated from our tunneling data are 20–40% too high. This does not change our overall conclusions since the discrepancies we discuss later are much larger. Also our T-dependent data are in good agreement with break junction work, for example Fig. 1 of Ref. [12]. This rules out possible effects from a parallel conductance path with a strong T dependence that were suggested by one referee.

In the following we consider 0.16 and 0.11 as upper and lower limits to the residual DOS obtained from heat capacity and microwave studies. Previously we ascribed [16] this residual term to pairs being broken around the nodes. But it is ruled out within the Dynes formulation used here because for a cylindrical Fermi surface with a residual DOS, $\delta n(0)/n(0)$, in the range 0.11 to 0.16, there would have to be broken

pairs over an angular range $\pm\alpha$ around each node with α ranging from 5 (0.11×45) to 7.2 (0.16×45) degrees. With $M^2 \propto (\cos 2\theta)^4$ there is a large attenuation factor given by $\int_0^\alpha \sin(2\alpha)^4 d\alpha / \int_0^{\pi/4} \sin(2\alpha)^4 d\alpha$, which ranges from 0.52 to 3.3×10^{-4} for these values of α. The contribution from incoherent tunneling between nodes would be larger, ranging from $(0.11)^2 \times 0.2$ to $(0.16)^2 \times 0.2$, but still a factor of 5 to 2 smaller that our experimental value of $G_S(0)/G_N(0) = 0.012$. The above estimates lead to the conclusion that the residual conductance, specific heat, and unpaired electron states are associated with non-nodal regions. They must have larger values of Γ, but are not necessarily completely normal, and seeing them in ARPES data might be hampered by the bilayer splitting. One intriguing possibility is that they are associated with the "hot spots" where the antiferromagnetic wave vector $\mathbf{Q} = (\pi/a, \pi/a)$ spans the Fermi surface. Namely electron states separated by $\mathbf{Q}$ are (a) strongly scattered by spin fluctuations and (b) must themselves combine in order to give rise to spin fluctuations at this wave vector, in the same way that electron states separated by a nesting vector combine to give a charge or spin density wave. We note that the residual specific heat of YBCO crystals is very similar [41–43] and is also not understood. Adding the residual value of $G_S(0)/G_N(0) = 0.012$ to the calculated $G_S(V)$ curve in Fig. 2(b) is justified within this picture because at low V the calculated curves are dominated by near-nodal contributions.

However high-quality mesa data taken over 18 years ago [34] and analyzed theoretically [34–36] *was* interpreted in terms of pair breaking at the nodes. In this theory, in the completely coherent limit, broken pairs near the nodes give a quasiparticle conductivity at zero bias given by:

$$\sigma_q = 2(e^2/\hbar)t_\perp^2 N(0)s/(\pi \Delta_0). \tag{3}$$

Here, in the notation of Ref. [34], $t_\perp$ is the c-axis tunneling parameter at the nodes, $N(0)$ is the 2D carrier DOS per spin direction in the normal state, and $s = 15.2 \times 10^{-8}$ cm is the interlayer spacing. In Ref. [34] the additional incoherent contribution to σ_q was found to be negligible for much smaller levels (10%) of coherence so we are justified in neglecting it here. In contrast to the Dynes formulation, the scattering rate does not affect σ_q because of cancellation between an increase in DOS near the nodes caused by scattering and a decrease in the tunneling probability associated with the broadening of the quasiparticle spectral function $A(\mathbf{k}, E)$. This tunneling probability effect is absent in Eq. (1). Experimentally σ_q is in the range 1–3 $(\text{k}\Omega\,\text{cm})^{-1}$, as indeed it is in our mesas, specifically $\sigma_q = 1.6$ $(\text{k}\Omega\,\text{cm})^{-1}$ for OD80. However in contrast to Ref. [34] we believe that $t_\perp$ must be angle dependent, because setting $\sigma_q = 1.6$ $(\text{k}\Omega\,\text{cm})^{-1}$ in Eq. (3) gives a very low value for $\langle t_\perp^2 \rangle = 8.4 \times 10^{-4}$ meV^2. This is much smaller than what is expected from the electrical resistivity and its anisotropy at 300 K, $\rho_{ab} = 0.22$ mΩ cm and $\rho_c = 1.8$ Ω cm [20,45]. Work on anisotropic organic conductors [45,46] suggests that in situations where the in-plane conductivity is described by the usual band theory and the out-of-plane conductivity is via tunneling, the formula for resistivity anisotropy (A) is the same [47] to within a factor 2, as that given by standard Boltzmann transport theory, namely $A = \langle v_\parallel^2 \rangle / \langle v_\perp^2 \rangle$, where $v_\parallel$ and $v_\perp$ are the in- and out-of-plane Fermi velocities, respectively. Taking

the Fermi surface of Bi-2212 to be a warped cylinder with tight-binding dispersion in the c direction, using $v_\parallel = 1.6 \times 10^7$ cm/sec and $A = 8200$ gives $\langle t_\perp^2 \rangle = 0.28$ meV^2. There is some uncertainty here because our mesa data gives larger values of $\rho_c = 8.1$ Ω cm at 300 K, corresponding to $\langle t_\perp^2 \rangle = 0.064$ meV^2.

The large difference between the value of $\langle t_\perp \rangle$ given by Eq. (3) for $\sigma_q = 1.6$ $(\text{k}\Omega\,\text{cm})^{-1}$ and the value from the resistivity anisotropy at 300 K is consistent with M being highly anisotropic. But as mentioned already, for a cylindrical Fermi surface with a residual DOS between 0.11 and 0.16, the attenuation from the $M^2 \propto (\cos 2\theta)^4$ factor ranges from 5.2×10^{-5} to 3.3×10^{-4}. So even for the larger value $\langle t_\perp^2 \rangle = 0.28$ meV^2, σ_q given by Eq. (3) is still a factor of 58 to 9 too low. To summarize, if we apply Eqs. (1) and (2) then we would conclude that the residual conductivity and DOS mainly arises from low-energy states well away from the nodes, a conclusion hinted at in H-dependent specific heat work [41]. Further evidence against significant pair breaking near the nodes comes from ARPES data for OD80, for example from Fig. 2(c) of Ref. [1] we estimate that any quasinormal region is less than ± 3 degrees around each node. More calculations may be needed regarding broken pairs near the nodes because in Ref. [34] the data were analyzed in terms of strong (resonant) scattering and a large pair breaking parameter $\gamma \sim 0.1\Delta_0$. There is evidence from subsequent microwave studies [40] that weaker, small-angle scattering from out-of-plane defects may be dominant in Bi-2212 crystals.

We note that the structure above the gap edge for OD78 and OP86 in Fig. 2(a) is smaller than for OD80. We suggest that this is not an intrinsic effect, namely it arises from small (10%) variations in the resistance of junctions within a stack. As can be seen from Fig. 1, several of the red I-V curves for OP86 and OD78 have lower values of I than the blue scaled curves for the same values of V, i.e., their resistances are at least 10% higher. Figure 3 shows that if three junctions out of 10 have 10% higher resistance then this nonuniformity has a strong effect on the depth and shape of the dip above the gap. We believe that this is the main reason for a certain lack of reproducibility in this structure from one ITJ to another [16,26].

IV. MAGNETIC FIELD DEPENDENCE

A. At zero bias

The quasiparticle DOS produced by a magnetic field in a d-wave superconductor at low T, is predicted [48] to be $N(H) \sim n(0)[H/H_{c2}(0)]^{1/2}$, where $H_{c2}(0)$ is the upper critical field as $T \to 0$ and $n(0)$ is the electronic DOS at the Fermi energy in the normal state. This pair breaking effect arises from Doppler shifts in the energies of $+\mathbf{k}$ and $-\mathbf{k}$ states caused by the superfluid flow around the vortices in the vortex state. For low H, pairs are broken near the nodes, where the superconducting gap is small, but the region widens as H is increased. The effect is seen in heat capacity studies of YBa$_2$Cu$_3$O$_7$ crystals, for example Ref. [41]. We estimate $H_{c2}(0) \parallel c$ for OD80 using the clean limit formula $H_{c2} = 0.59\Phi_0/[2\pi \xi_{ab}(0)^2]$ given in Ref. [23], where Φ_0 is the flux quantum for pairs and $\xi_{ab}(0)$, the in-plane superconducting coherence length as $T \to 0$, equals $\hbar v_F/[\pi \Delta(0)]$. Here v_F is the Fermi velocity and $\Delta(0)$ the superconducting gap parameter as $T \to 0$. We estimate $v_F = 1.58 \pm 0.12 \times 10^7$ cm/sec by applying a simple
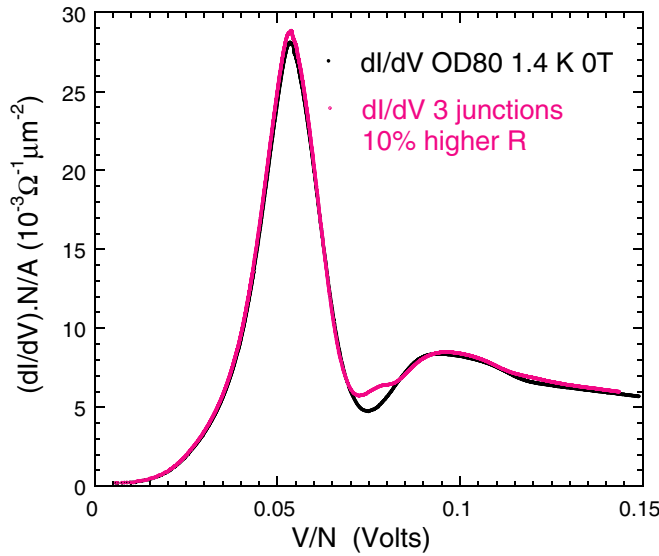
FIG. 3. Calculation showing sensitivity of structure above the gap edge to the resistance of individual junctions. The black curve corresponds to the case where all 10 junctions have the same resistance and dI/dV as measured for the best ITJ OD80. The purple curve shows the effect of having three out of 10 junctions with 10% higher resistance, i.e., 10% larger values of V for the same I.

FIG. 4. Zero bias conductance for the three mesas at 1.4 K obtained from straight line fits to I/V vs V^2 curves, for V typically between 0.009 and 0.012 V, at various fields, H applied along the c axis. The normal state conductance at zero bias $G_N(0)$ is obtained from the polynomials that give states-conserving fits, see Ref. [38]. The dashed lines show fits for 20% incoherent tunneling of unpaired quasiparticles near the nodes in one layer, generated by the Volovik effect, to zero energy non-nodal states in the neighboring layer (see text).

cylindrical Fermi surface model to quantum oscillation data [49] for overdoped Tl2201 crystals for which the doping-independent effective mass is $5.2 \pm 0.4 m_e$. Taking the measured value $\Delta(0) = 26.9$ meV at the antinodes for our OD80 Bi-2212 mesa, and applying the above formulas, which may contain extra constants of order unity for d-wave rather than s-wave pairing, gives $\xi_{ab}(0) = 12.3 \pm 0.9 \times 10^{-8}$ cm and $H_{c2}(0) = 128 \pm 20$ T. By analyzing specific heat data for YBa$_2$Cu$_3$O$_7$ crystals the authors of Ref. [41] found $N(H)/n(0) = a\sqrt{8H/[\pi H_{c2}(0)]}$, where experimentally the constant $a = 0.7 \pm 23\%$. According to this formula and the above value of $H_{c2}(0)$ we would expect the field-induced DOS to be $36 \pm 9\%$ of the normal state value $n(0)$ at 13 T. Plots of $G_S(0)/G_N(0)$ vs H for the three mesas are shown in Fig. 4. They all have the same general shape and magnitude, both of which agree rather well with previous ITJ experiments [35]. However the increase in $G_S(0)/G_N(0)$ between 0 and 13 T, $\simeq 0.01$, is very small compared with the $36 \pm 9\%$ increase in DOS predicted by the theory of Volovik [48]. In Refs. [35] and [36] this was ascribed to cancellation between the increased DOS and the increased scattering of quasiparticles on vortices, when vortex pancakes in adjacent layers are uncorrelated.

The above estimates of the constant a and $H_{c2}(0)$ show that for a cylindrical Fermi surface, at 13 T pairs should be broken over an angular range of $0.36 \pm 0.09 \times 45 = 16.2 \pm 4.0$ degrees either side of a d-wave node. We have considered three simpler interpretations of the H dependence in Fig. 4, (i) coherent tunneling, (ii) incoherent tunneling, both between nodal regions in neighboring layers, and (iii) incoherent tunneling between a nodal region in one layer and non-nodal regions in the neighboring layer. We use the same coherence/incoherence ratio (4:1) as before. Because of the $M^2 \propto (\cos 2\theta)^4$ factor, case (i) gives a very wide range of values for the increase
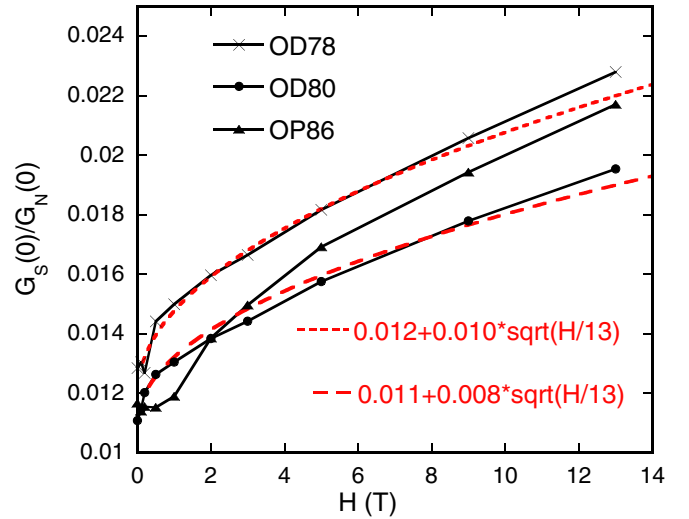
in $G_S(0)/G_N(0)$ from 0 to 13 T, the upper limit (0.007) is somewhat lower than the experimental value, and the H dependence, dominated by the $M^2 \propto (\cos 2\theta)^4$ factor, is completely wrong. Case (ii) gives values which are too high by a factor of 2.7 ± 1.3 and a linear H dependence. Case (iii) gives very good agreement with experiment both in magnitude and H dependence as shown by the dashed lines in Fig. 4, namely the increase in $G_S(0)/G_N(0)$ between 0 and 13 T is 0.010 ± 0.004 and is proportional to $H^{1/2}$. The rather large error arises from the uncertainty in the constant a in the formula used for the Volovik DOS, and the uncertainty in the residual DOS at $H = 0$. We note that case (iii) implicitly assumes that the vortex pancakes in neighboring layers are uncorrelated, and this fact would suppress the nodal-nodal contributions in cases (i) and (ii) which might otherwise be significant. So, somewhat surprisingly, the Dynes formulation used here plus the assumption that there is 20% incoherent tunneling to zero-energy states well away from the nodes, seems to give a good description of the H dependence of $G_S(0)/G_N(0)$.

B. At higher bias

Figure 5(a) shows dI/dV per unit area for one junction of OD80, at 1.4 K vs the bias voltage per junction, for many fields $H = 0$ to 13 T applied perpendicular to the CuO$_2$ planes. The curves are symmetric for $\pm V$, so for clarity we only show data for $V > 0$. For such SIS junctions the sharp peaks are located at voltages of $2\Delta_0/e$, where Δ_0 is the maximum value of the d-wave gap. At 1.4 K this gives $\Delta_0 = 27.3$, 26.9, and 27.4 meV for the three mesas studied here, OD78, OD80, and OP86, respectively, in good agreement with the lower values shown in Fig. 15 of Ref. [2] for these doping levels. The ratio
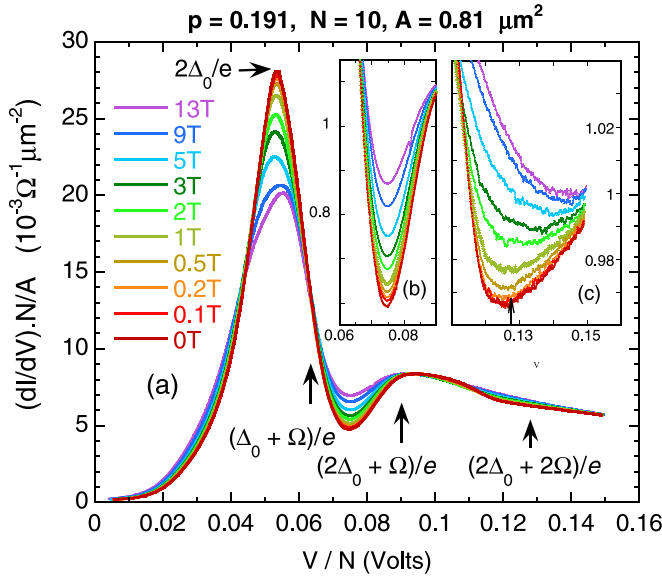
FIG. 5. (a) dI/dV curves for OD80 at 1.4 K in various magnetic fields applied perpendicular to the CuO_2 planes plotted vs V/N, the bias voltage per junction. Numerical data is available [44]. (b) and (c) show details of the field dependence of the lower and upper dips. Here dI/dV curves have been normalized by dividing through by the polynomial given in Ref. [38]. Values of $(\Delta_0 + \Omega)/e$, $(2\Delta_0 + \Omega)/e$, and $2(\Delta_0 + \Omega)/e$ are shown by arrows (see text).

$2\Delta_0/k_B T_c = 8.08 \pm 0.1$, 7.83 ± 0.1, and 7.5 ± 0.15 for these three mesas is ∼1.75–1.9 times larger than for a weak-coupling d-wave superconductor [25].

The dI/dV data for OD80 in Figs. 5(a)–5(c). show two H-dependent dips above $eV = 2\Delta_0$. (Data in Figs. 5(b) and 5(c) have been normalized, see Ref. [38]). For a d-wave energy gap varying as $\Delta_0 \cos 2\theta$, where θ is the angle between **k** and the antinodal direction, and for a dispersionless (**k**-independent) boson energy Ω, boson-induced structure is expected to be most apparent at $eV = 2\Delta_0 + \Omega$. At this bias voltage, states at the gap edge at Δ_0 for $\theta = 0$ on one side of the junction and any structure at $\Delta_0 + \Omega$ and $\theta = 0$ on the other side are aligned to the same energy, and strong tunneling occurs between these. The effect is largest there because the peak in the superconducting d-wave quasiparticle DOS is largest at $\theta = 0$. Additional structure is expected near $eV = 2\Delta_0 + 2\Omega$ where boson-induced anomalies on each side of the junction at $\theta = 0$ have the same energy. However, for a reasonably isotropic Fermi surface (without a substantial Van Hove singularity as discussed earlier) we would expect this structure to extend to lower energies since at other angles in **k** space, $2\Delta_\mathbf{k} + \Omega$ will be smaller.

The $S = 1$, magnetic resonance excitation, seen by inelastic neutron scattering [50], is a candidate pairing boson [30,51]. It has an energy $\Omega = 5.4k_B T_c$ [30,50] and a momentum vector **Q**, close to $(\pi/a, \pi/a)$, [30,50] where a is the in-plane lattice spacing. Various energies associated with this value of Ω are shown in Figs. 5 and 7 for OD80. It can be seen that there is a rough correspondence with the simple description given above. In view of the Volovik effect, the interpretation of the strong H dependence which we proposed in Ref. [16] was that nodal quasiparticles were having a strong effect on
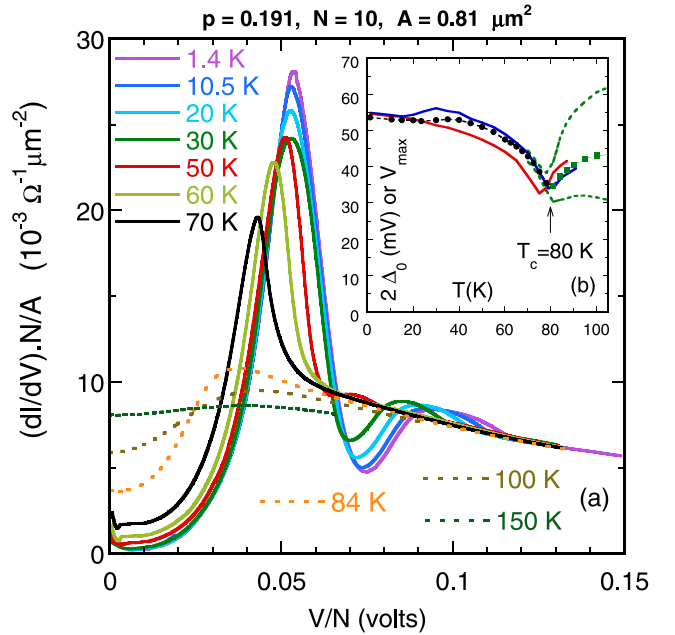

FIG. 6. (a) dI/dV curves for OD80 at selected values of T. Numerical data for 31 values of T between 1.4 and 300 K is available [44]. (b) T dependence of the d-wave gap $2\Delta_0(T)$ up to T_c from the main peaks in dI/dV for OD80 (black circles), OD78 (red squares), and OP86 (blue triangles). For OD80, green squares above $T_c = 80$ K give voltages of broad maxima in dI/dV. Green dashed lines show their increased breadth by marking regions where $dI/dV \geqslant 0.95(dI/dV)_{MAX}$.

the structure above the gap edge. This is still a possibility but we cannot rule out a much more prosaic interpretation in which the disorder associated with having uncorrelated vortex pancakes in neighboring layers [35,36] smooths out this structure. Quasiparticles tunneling from regions between vortices in one layer (where in the first approximation the gap parameter will be the same as at $H = 0$) to vortex cores in the next layer will give different contributions to the I-V curve that depend on the interlayer vortex correlations. If the vortex cores are uncorrelated this statistical effect will tend to smooth out the structure above the gap in a similar way to the effect of resistance variations shown in Fig. 3. In support of this latter scenario we note that the dip in optimally-doped Bi-2212 SIS break junctions [52] was not suppressed by fields of up to 12 T parallel to the c axis. Also recent STM work [53] on YBCO shows the presence of dips in applied fields of up to 6 T ∥ c though in the diagrams shown they are rather small.

V. TEMPERATURE DEPENDENCE

A. Below T_c

Figure 6(a) shows the overall T dependence of our raw dI/dV data for OD80 in zero field at selected temperatures, while data for a total of 31 temperatures below and above T_c are given as Supplemental Material [44]. The data in Figs. 6(a) and 7 show that the dip and the hump at higher V are strongly T dependent and have almost disappeared at 50 K even though Δ_0 has hardly changed from its low T value there. The attenuation of the hump is much smaller up to 40 K, but it shifts down
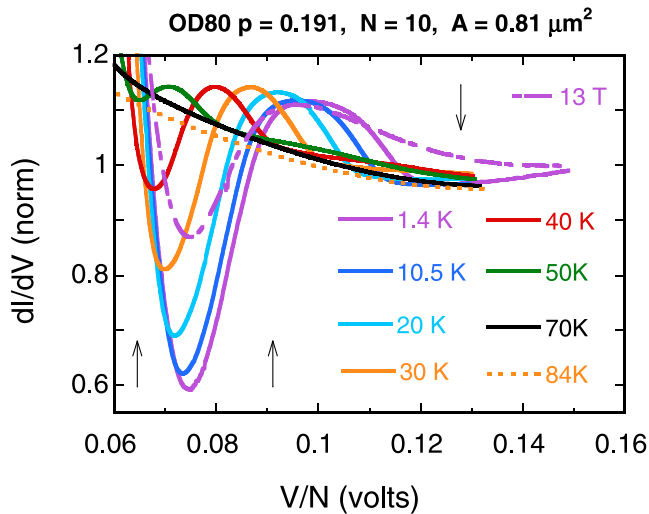
FIG. 7. Zoom of the structure above the gap edge for OD80 at selected T. The data have been normalized for clarity, see Ref. [38]. Values of $(\Delta_0(0) + \Omega)/e$, $(2\Delta_0(0) + \Omega)/e$, and $2(\Delta_0(0) + \Omega)/e$ are shown by arrows (see text). Data at 1.4 K for a magnetic field of 13 T $\parallel c$ are also shown.

with increasing T and also disappears rapidly between 50 and 60 K. We feel that this strong T dependence, especially the shifts of the dips and humps with T, is unlikely to be caused by a conventional phonon pairing mechanism. As shown in Fig. 7, the lower dip is partially suppressed by a magnetic field, but it is not shifted, unlike the effect of temperature. For all three mesas a relatively sharp fall in $2\Delta_0(T)$ also sets in just above 50 K as shown in Fig. 6(b). A striking feature of Fig. 6(b) is that just below T_c, $2\Delta_0(T) \simeq \Omega = 5.4 k_B T_c$, possibly suggesting that the integrity of the magnetic mode is essential for superconductivity [30].

The dI/dV curves in Fig. 6(a) *above* T_c also have peaks whose breadth increases rapidly with T as indicated by the green dashed lines for OD80 in Fig. 6(b). They appear to be states-conserving, for example at 84 K the polynomial normalization used earlier gives a dI/dV curve that conserves states to within 2.2% for the range of V shown in Fig. 6(a). The presence of these broad peaks for $p = 0.19$ agrees with a laser ARPES study [1] of Bi-2212 showing a pseudogap above T_c extending up to $p = 0.22$. However in a later section we show that for OD80 and presumably for the $p = 0.19$ crystal studied by ARPES [1], the pseudogap above T_c is consistent with the effect expected from superconducting fluctuations [23]. In contrast the "real" pseudogap, which we believe to be an energy scale, sets in abruptly [1] below $p = 0.19$ in agreement with earlier heat capacity [19] and penetration depth [21,22] measurements and is not expected to be visible in our data for OD80. Furthermore, in contrast to the gap above T_c discussed here, the "real" pseudogap is not states-conserving [19].

As recognized previously [2,12], the T dependence of the data in Fig. 6(a) at all bias voltages below 0.12 V cannot be ascribed simply to thermal broadening. In Ref. [16] we argued that this could be shown in a model-independent way by comparing measured dI/dV curves at a given T with the 1.4 K curve smoothed over an appropriate voltage range corresponding to $eV = 5.6 k_B T$. However calculations

using Eq. (2) at various temperatures do not support this procedure, so in Figs. 8(a)–8(e) we show instead comparisons of our data with Eq. (2) at selected values of T. The calculated curves all have the same (E-dependent) values of $\Gamma = 0.009 + 0.07x^4/(1 + x^2)$, used in Fig. 2(b), but now $x = E/\Delta_0(T)$, with $\Delta_0(T)$ given in Fig. 6(b). In Fig. 8(f) we show the effect of extra E-independent damping values, i.e., $\Gamma = \gamma + 0.07x^4/(1 + x^2)$ with γ ranging from 0.09 to 0.3. Figure 8 highlights the fact that the peaks at $2\Delta_0(T)$ become narrower at the same temperature, near 50 K, where the dip-hump structure is strongly attenuated. It implies that below 50 K this structure and the broadening have a common origin, namely renormalization from the pairing boson(s).

In Figs. 8(d) and 8(e) the upturn in the Dynes calculation near $V = 0$ is clearly seen, This is well known in classical SIS tunneling work [9] and arises from the thermal population of quasiparticle states above and below the gap edge when $\Delta \sim k_B T$. But the experimental data show an important difference in that $G(V)$ remains constant up to larger voltages $\sim 0.02 V$ than the calculated curves before merging smoothly with them. This must mean that Γ is relatively large where Δ is large and where M is only weakly dependent on θ. We are therefore justified in estimating a scattering rate Γ from the relation $G_S(0,T)/G_N(0) = \Gamma^2/\Delta_0(T)^2$. The T dependence of $G_S(0)/G_N(0)$ was obtained by fitting I-V curves at all temperatures measured to $I/V = m_1 + m_2 V^2$ typically from 0.01 to 0.014 Volts and normalizing m_1 to the normal state using states-conserving polynomials [38]. The results are shown in Fig. 9 on a semilogarithmic scale to emphasize the behavior at low T. Normalized data for the three mesas are in excellent agreement, the data for OD78 and OD80 obey an $A + BT^4$ law, while for OP86, $A + BT^3$ gives a marginally better fit. A T^3 power law was obtained earlier, using much larger 20×20 μm^2 mesas, but employing a pulse method to reduce heating effects and suppressing Josephson currents with a 1 T applied field [54]. Figure 9 is appropriate for two types of comparison with theory. Firstly, as mentioned above, in Eq. (3), the scattering rate does not affect $G_S(0)$ and so in this case the main T dependence will presumably come from the fact that normal regions around the nodes expand as T increases causing M to increase strongly with T. However in contrast to the assumption in Ref. [34], analysis of microwave conductivity data [40] points towards the importance of small-angle scattering processes so this aspect would need to be addressed. Secondly it has been suggested that thermodynamic fluctuations are extremely important in Bi-2212 [55]. In this case one might expect the activation energy for two-dimensional fluctuating normal regions at low T to be given by $E_A = \Delta F_{NS} \xi_{ab}(0)^2 s$ where ΔF_{NS} is the difference in free energy densities at $T = 0$ (the superconducting condensation energy density, U), $\xi_{ab}(0)$ is the in-plane coherence length at low T, and s is the interplanar spacing. Taking $\Delta F_{NS} = 1.9$ J/gm.at [19], $\xi_{ab}(0) = 12.8 \times 10^{-8}$ cm, and $s = 15.2 \times 10^{-8}$ gives $E_A/k_B = 40$ K, of the same order, and actually a factor of 3–4 less than the values obtained from the Arrhenius fits shown in Figs. 9(b) and 10(b). However we argue later that our data for OD80 above T_c are consistent with weaker superconducting fluctuations which goes against this interpretation.

As argued above, within the Dynes formulation used here, the scattering rate Γ is given by $\sqrt{G_S(0)/G_N(0)}\Delta_0(T)$ and
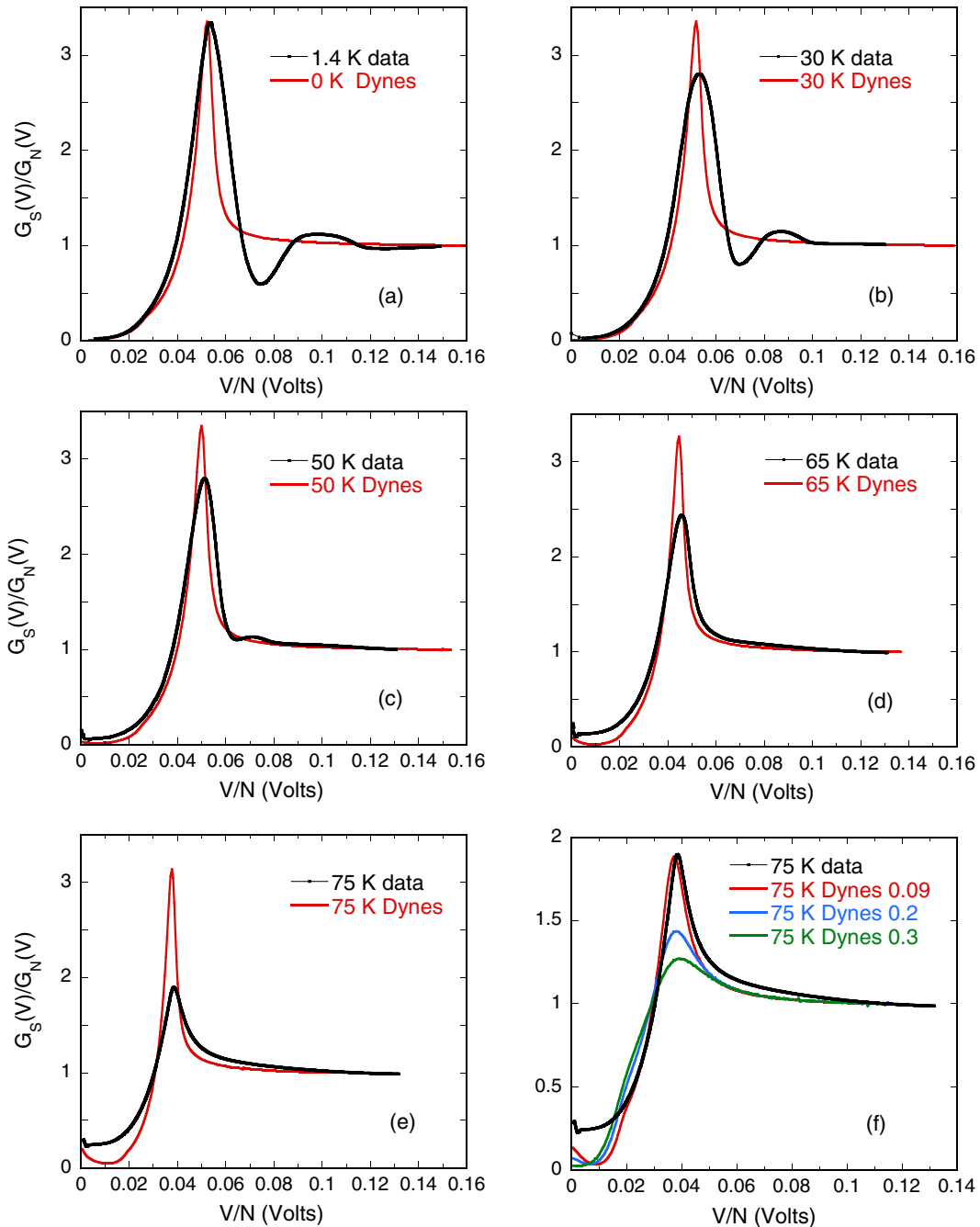
FIG. 8. (a)–(e) Comparison of normalized dI/dV curves with the Dynes formula Eq. (2), with a 4:1 coherence-incoherence ratio, and the same damping factor, $\Gamma = 0.009 + 0.07x^4/(1 + x^2)$ where $x = E/\Delta_0(T)$, at the selected temperatures shown. (f) Effect of various extra dampings, $\Gamma = 0.09 + 0.07x^4/(1 + x^2)$ etc. at 75 K.

appropriate plots are shown in Figs. 10(a) and 10(b). Figure 10(a) shows the data for the three mesas together with fits to an empirical formula describing inelastic scattering between quasiparticles which is expected to vary as T^4 at low T and then cross over to T^2 as $2k_B T$ becomes comparable with the maximum superconducting energy gap $\Delta_0(T)$. This formula gives a good fit to the data but the crossover temperature $\sim$50 K corresponding to $2k_B T = \Delta_0(T)/3$ could be rather low, and a more precise calculation is needed. Figure 10(b) shows Arrhenius fits to the scattering rate. The values of E_A

are $\sim$12 meV for all three mesas. This is reasonably close to the energy difference between the $S = 1$ resonant mode at $5.4k_B T_c = 37$ meV for OD80 and the value $2\Delta_0 = 54$ meV. So another possible interpretation of the activated behavior is that it represents thermally induced decay of the $S = 1$ resonant mode into the quasiparticle continuum above the gap edge. It could be argued that for a d-wave superconductor the gap edge extends down to zero energy at the nodes. But decay processes there would be restricted by **k** conservation and the fact that the $S = 1$ mode has a reasonably well-defined **Q**
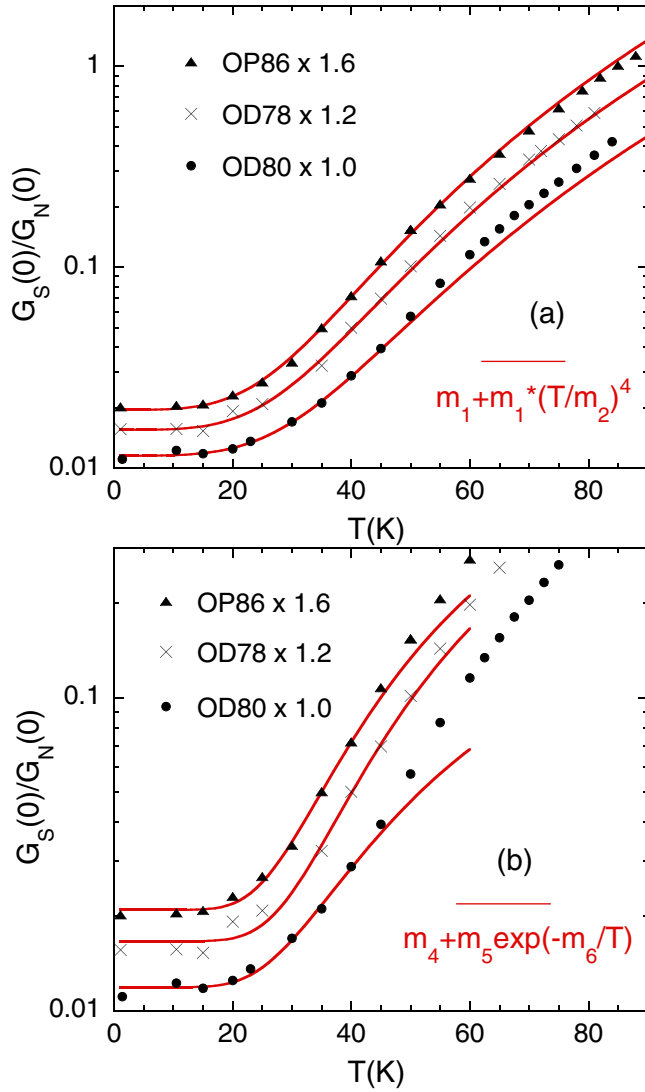
FIG. 9. Values of $G_S(0)/G_N(0)$ vs temperature for the three mesas. (a) shows the data together with fits to $m_1 + m_1(T/m_3)^4$ with $m_1 = 0.0129$, 0.0115, and 0.0122 and $m_3 = 33$, 36, and 31 K for mesas OD78, OD80, and OP86, respectively. (b) shows the same data and fits to the Arrhenius law shown with $m_4 = 0.0139$, 0.0119, and 0.0131, $m_5 = 2.60$, 0.65, and 1.67, $m_6 = 182$, 158, and 147 K for mesas OD78, OD80, and OP86, respectively. All fits have been made from 1.4 to 40 K. For clarity the data for OD78 and OP86 have been displaced along the logarithmic y axis by the multiplying factors shown.
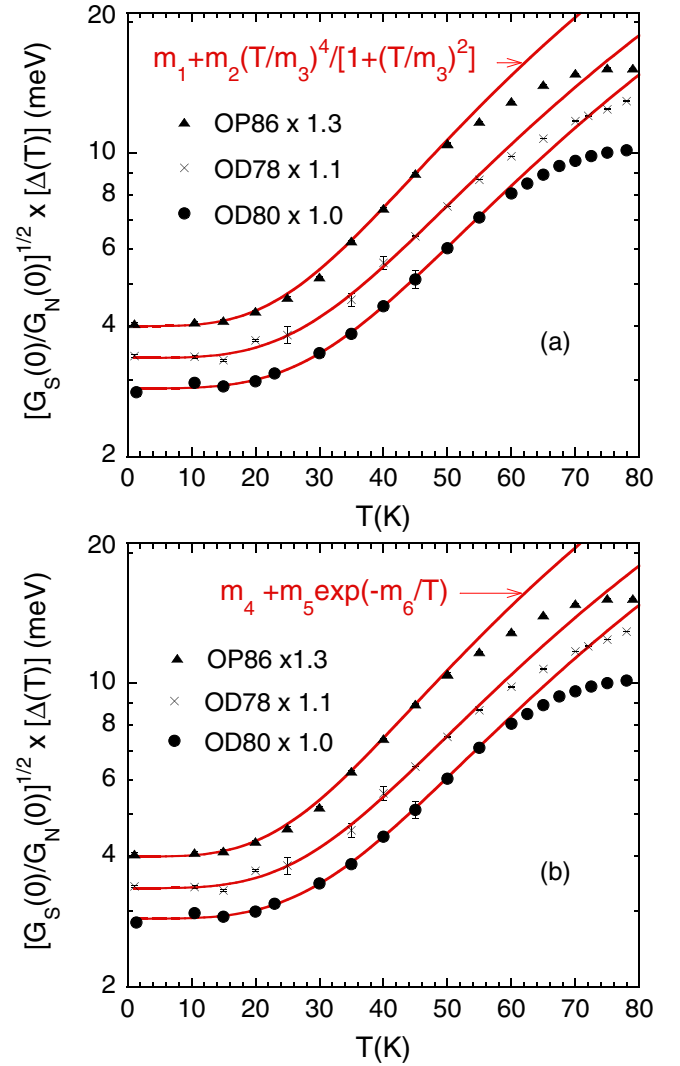

FIG. 10. Values of $\Gamma(T) \equiv \sqrt{G_S(0)/G_N(0)} \times [\Delta_0(T)]$ vs temperature for the three mesas. (a) shows the data together with fits to the formula shown that is expected for electron-electron scattering with $m_1 = 3.07$, 2.89, and 3.07 meV, $m_2 = 7.1$, 8.5, and 6.2 meV, $m_3 = 50$, 55, and 42 K for mesas OD78, OD80, and OP86, respectively. (b) shows the same data and fits to the Arrhenius law shown with $m_4 = 3.13$, 2.91, and 3.16 meV, $m_5 = 56$, 49, and 64 meV, $m_6 = 136$, 139, and 128 K for mesas OD78, OD80, and OP86, respectively. All fits have been made from 1.4 to 50 K. For clarity the data for OD78 and OP86 have been displaced along the logarithmic y axis by the multiplying factors shown.

vector near $(\pi/a, \pi/a)$. Figure 10 shows that $\Gamma \sim 8$–10 meV at 60 K for all three mesas including OP86. For comparison the scattering rate deduced [40] from the microwave conductivity of an OP88 Bi-2212 crystal is $\simeq 3 \times 10^{12}$ sec^{-1} at 60 K or 2 meV. From this we conclude that the microwave studies are sensitive to lifetimes nearer the nodes while, because of the strong angle dependence of M, our tunneling data picks up lifetimes nearer the antinodes. This could also be the reason why the T dependence in Fig. 10 at low T is much flatter than in the microwave studies, e.g., Fig. 4 of Ref. [40]. In general, if real quasiparticle-boson scattering processes are responsible for Γ then its T dependence will be related to the boson DOS.

We see from Fig. 10 that the scattering rate for states near the antinodes is 10–12 meV as T_c is approached from below, while from Fig. 6(b) $\Delta_0(T \to T_c) \sim 16$–17 meV. We therefore conclude that the larger values of dI/dV at low V, i.e., $(dI/dV)_{res}$ are caused by T-dependent pair-breaking processes in line with early break junction work [12]. The scattering rates are surprisingly large and must be connected in some way with the fact that as shown in Fig. 6(b) $\Delta_0(T \to T_c)$ is also large, possibly suggesting that T_c is suppressed by inelastic scattering. The same general viewpoint was proposed by us in Ref. [16] as well as in two ARPES papers [56,57] that have inspired a detailed comparison [58] of ARPES data
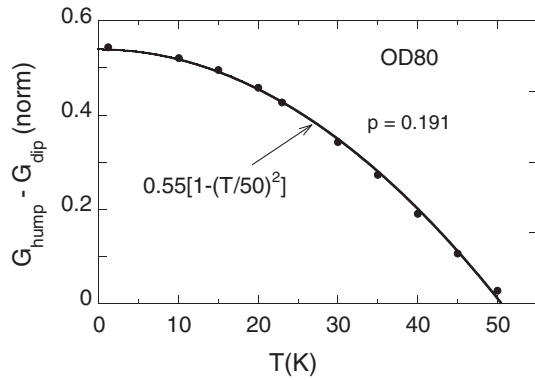
FIG. 11. T dependence of the difference between the maximum of dI/dV at the hump and the minimum at the dip for OD80. The points have been obtained from normalized dI/dV curves such as those shown in Fig. 7. The data show a clear T^2 dependence that goes to zero at 50 K.

with several bulk properties. But, in contrast to these last three papers, we believe that the gap above T_c in OD80 can be understood reasonably well in terms of the accepted theory [23] of superconducting fluctuations, as explained below.

Finally, to conclude this section, in Fig. 11 we show that the amplitude of the dip-hump feature for OD80 obeys an $A - BT^2$ law to high accuracy, becoming almost zero at 50 K. Again this seems to be completely at odds with expectations for electron-phonon scattering. Data for the other two mesas do not show this behavior but in contrast to Ref. [16] we now ascribe this to the interlayer conductance of OD80 being more uniform than for the other two mesas.

B. Above T_c

The dI/dV data for mesa OD80 at all temperatures measured above T_c [44] are shown in Fig. 12(a) and data at higher T, normalized as explained in Ref. [38], are shown in Fig. 12(b). The theory of superconducting fluctuations [23] predicts that in the 2D limit the fluctuation contribution to the tunneling conductance of an NIS junction at $V = 0$ is given by:

$$G_{\text{FL}}(0,T)/G_N(0,T) = -2\tau_G \ln(1/\epsilon), \quad (4)$$

where $G_N(0,T)$ is the conductance in the normal state in the absence of fluctuations, τ_G is the Ginzburg parameter, and $\epsilon = \ln(T/T_{\text{MF}})$, where T_{MF} is the mean field superconducting transition temperature (at which the first term in the Ginzburg-Landau free energy expansion changes sign from positive to negative). The voltage dependence of the fluctuation contribution is given in terms of the second derivative of the digamma function Ψ by [23]:

$$G_{\text{FL}}(V,T) \propto G_{\text{FL}}(0,T) Re\left[\Psi''\left(\frac{1}{2} - i\frac{eV}{2\pi k_B T}\right)\right]. \quad (5)$$

Equation (4) shows that, unusually, the fluctuation contribution to the conductance has a very weak T dependence because of the double logarithm while Eq. (5) shows that the voltage dependence extends to unexpectedly high voltages since $G_{\text{FL}}(V,T)$ has a positive maximum at $eV = \pi k_B T$. In order to make a detailed comparison with our data these equations
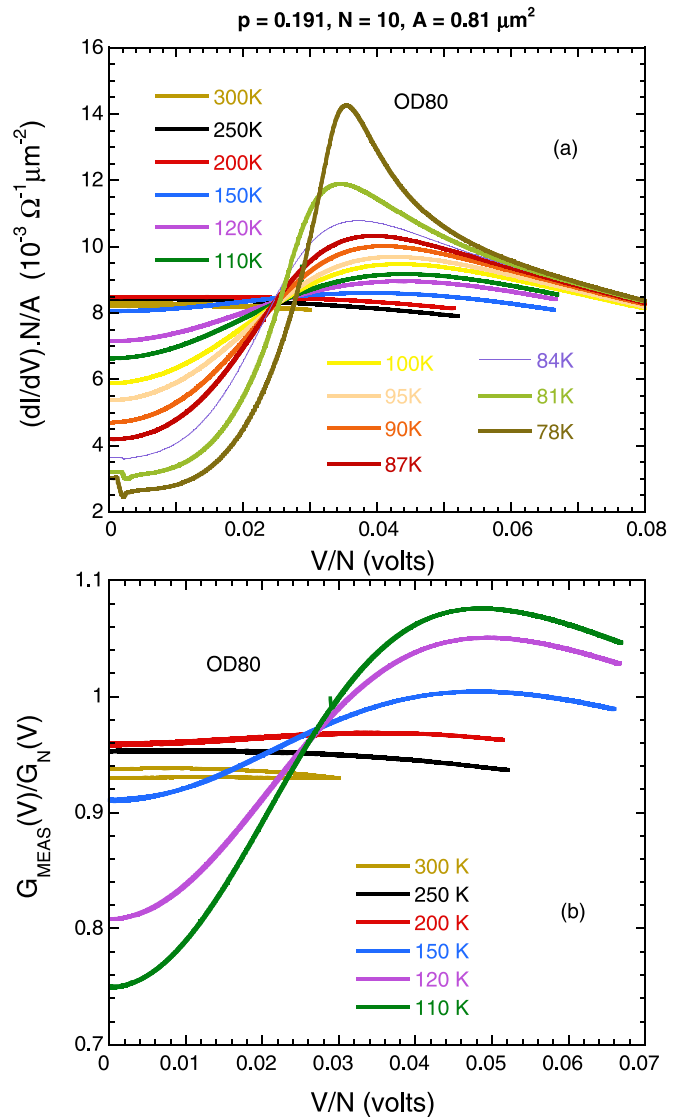

FIG. 12. (a) dI/dV curves measured for OD80 above T_c plus one curve at 78 K for comparison. Numerical data for 31 values of T between 1.4 and 300 K is available [44]. (b) Zoom of data measured for OD80 in the range 110–300 K, after normalizing by a polynomial that gives a states-conserving curve at 1.4 K and 13 T, see Ref. [38]. At higher T the sweep voltage range had to be restricted because of hysteresis associated with voltage-induced changes in the mesa resistance [59], as shown for example by the data at 300 K.

would need to be extended to the case of coherent tunneling between two d-wave superconductors with a tunneling probability $M^2 \propto (\cos 2\theta)^4$. But to within some numerical factors of order unity, for SIS junctions we would expect there to be an extra factor of 2 in $G_{\text{FL}}(0,T)/G_N(0,T)$ [23] and that the peak in $G_{\text{FL}}(V,T)/G_N(V,T)$ will occur at $eV = 2\pi k_B T$, a factor of 2 higher than for an NIS junction. Figure 13 shows the voltages of the maxima in $G_{\text{FL}}(V,T)/G_N(V,T)$ vs T on a log-log plot. The precise positions of the peaks are somewhat dependent on the normal state conductance and we show two limits for this. It can be seen that there is indeed a linear region between 87 and 110 K, and furthermore the slope (1.76) is reasonably close to 2.
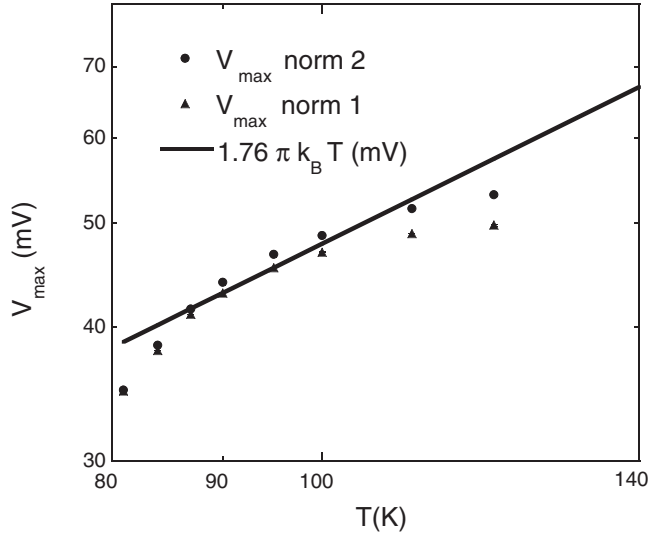
FIG. 13. Voltages of maxima in normalized dI/dV curves obtained from the data in Fig. 12, by fitting to $a + b(V - V_{\mathrm{max}})^2$ near the maxima. The linear T dependence expected [23] from superconducting fluctuation theory has unit slope on the logarithmic scales used. There is indeed a linear region with approximately the expected slope of $2.0\pi k_B$ between 87 and 110 K. Results are shown for two different normalizing polynomials [38].

We have examined the applicability of Eq. (4) by subtracting a normal state background contribution of the form $G_N(0,T) = 1/(a + bT)$ where a and b are constants fixed by our two measured points at 250 and 300 K, but a quadratic form $G_N(0,T) = a + bT^2$ with a fixed by the first term (8.85) in the polynomial used for normalizing $G_S(V, 1.4K)$, and b by the 300 K data point gave very similar results. The raw data and the $G_N(0,T) = 1/(a + bT)$ background are shown in Fig. 14. The normalized values $|G_{\mathrm{FL}}(0,T)|/G_N(0,T)$ obtained from Fig. 14 are plotted vs $\ln[1/\ln(T/T_{\mathrm{MF}})]$ in Fig. 15 for three values of T_{MF}. Because of the weak dependence of the double logarithm on both T and T_{MF} we cannot use the quality of the straight line fits shown to determine T_{MF}. However, using Eq. (4) the slopes of the straight lines shown give values of the 2D Ginzburg temperature ranging from $\tau_G = 0.054$ for $T_{\mathrm{MF}} = 82$ K to 0.038
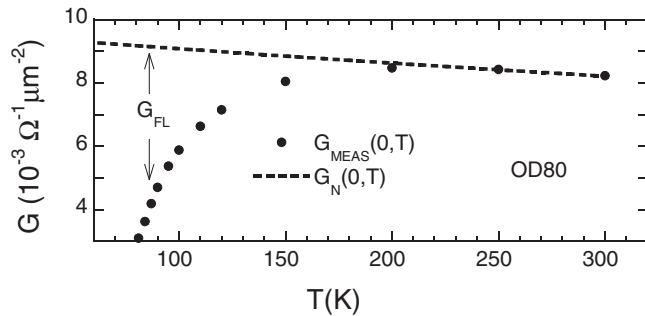

FIG. 14. Measured values of the zero-bias conductance vs T at all temperatures above T_c. The dashed line shows the estimated normal state conductance background $G_N(0,T)$ obtained by assuming that $1/G_N(0,T) = a + bT$ and finding a and b from the points at 250 and 300 K. The superconducting fluctuation part G_{FL} is also shown.
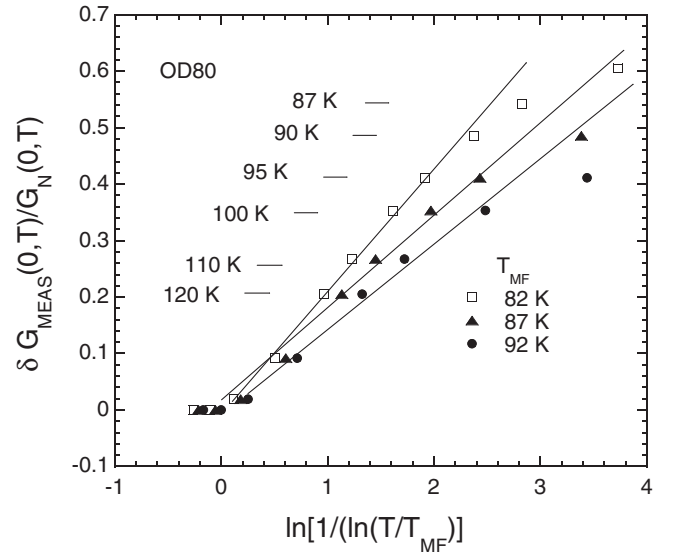

FIG. 15. Normalized values of the fluctuation contribution to the zero-bias conductance, $\delta G_{\mathrm{MEAS}} = [G_N(V=0,T) - G_{\mathrm{MEAS}}(V = 0,T)]/G_N(V=0,T)$, obtained from the data in Fig. 14, are plotted vs $\ln[1/\ln(T/T_{\mathrm{MF}})]$ for the three values of T_{MF} shown. The slopes of the lines shown give values of the Ginzburg parameter τ_G (see text).

for $T_{\mathrm{MF}} = 92$ K. The 92 K value is self-consistent in the sense that in the 2D case the suppression of T_c is given by [23]:

$$\frac{T_{\mathrm{MF}} - T_c}{T_{\mathrm{MF}}} = 2\tau_G \ln(1/(4\tau_G), \qquad (6)$$

and $\tau_G = 0.038$ corresponds to a suppression of 13 K. Because of possible uncertainty in numerical factors in Eq. (4) it is worth comparing this estimate of τ_G with that obtained from the superconducting condensation energy [19] and the 2D coherence volume mentioned earlier. The original definition of τ_G was in terms of the reduced temperature above T_c where the Gaussian fluctuation contribution to the heat capacity becomes as large as the mean-field jump that would occur in the absence of fluctuations [23]. For a classical superconductor with the usual parabolic dependence of the thermodynamic critical field $H_c(T) = H_c(0)[1 - (T/T_c)^2]$, the mean field specific heat jump at T_c is $H_c(0)^2/(\pi T_c)$ and setting this equal to the 2D Gaussian fluctuation term $k_B/(4\pi \xi_{ab}(0)^2 s \tau_G)$ at τ_G gives a formula that is probably more general and more suitable for the d-wave superconductor with a larger value of $\Delta(0)/(k_B T_c)$ considered here, namely:

$$\tau_G = \frac{k_B T_c}{32\pi U \xi_{ab}(0)^2 s}, \qquad (7)$$

where the condensation energy density $U = H_c(0)^2/(8\pi)$. For OD80 we find $U\xi_{ab}(0)^2 s = 40$ K, giving a smaller value $\tau_G = 0.02$ and from Eq. (6), a suppression in T_c of 10%. Therefore the line in Fig. 15 with $T_{\mathrm{MF}} = 87$ K is probably more appropriate than $T_{\mathrm{MF}} = 92$ K. Recently [18] the contrasting effects of parallel and perpendicular magnetic fields on underdoped ITJs were used to distinguish the pseudogap from the gap arising from superconducting fluctuations. These authors reached a similar conclusion regarding superconducting fluctuations but here we have made a more precise numerical comparison with

theory [23] for an overdoped ITJ where there is no evidence for a pseudogap.

VI. CONCLUSIONS

In summary we have reported intrinsic SIS planar tunneling data for three crystals of the cuprate superconductor Bi-2212 and discussed their field and temperature dependence. We believe that there is enough information in our data to assess the pairing contribution from the $S = 1$ magnetic mode that has $\mathbf{Q} \simeq (\pi/a, \pi/a)$ [30,50]. On the basis of our analysis using the Dynes equation we conclude that the residual specific heat and normal fluid fraction do not arise from nodal regions. We argue that inelastic scattering is large and probably anisotropic since our tunneling data, which are more sensitive to the antinodal regions, give scattering rates near 60 K that are approximately four times larger than those obtained by microwave studies [40]. We have discussed the temperature dependence of this scattering in terms of electron-electron scattering. However a more exciting possibility is that it is caused by the same excitations whose virtual exchange is providing the pairing "glue." We have shown that the tunneling gap above T_c persisting up to 150 K is reasonably consistent with the theory of superconducting fluctuations [23] for relatively small values of the 2D reduced Ginzburg temperature, $\tau_G = 0.02$. This is consistent with the Gaussian fluctuation analysis used for various cuprates [60] that crosses over smoothly to the critical region at approximately 1.02–1.1T_c.

[1] I. M. Vishik, M. Hashimoto, R.-H. He, W.-S. Lee, F. Schmitt, D. Lu, R. G. Moore, C. Zhang, W. Meevasana, T. Sasagawa, S. Uchida, K. Fujita, S. Ishida, M. Ishikado, Y. Yoshida, H. I. Eisaki, Z. Hussain, T. P. Devereaux, and Z.-X. Shen, Proc. Nat. Acad. Sci. **109**, 18332 (2012).

[2] Ø. Fischer, M. Kugler, I. Maggio-Aprile, C. Berthod, and C. Renner, Rev. Mod. Phys. **79**, 353 (2007).

[3] K. Fujita, C. K. Kim, I. Lee, J. Lee, M. H. Hamidian, A. Firmo, S. Mukhopadhyay, H. Eisaki, S. Uchida, M. J. Lawler, E.-A. Kim, and J. C. Davis, Science **344**, 612 (2014).

[4] E. H. da Silva Neto, P. Aynajian, A. Frano, R. Comin, E. Schierle, E. Weschke, A. Gyenis, J. Wen, J. Schneeloch, Z. Xu, S. Ono, G. Gu, M. Le Tacon, and A. Yazdani, Science **343**, 393 (2014).

[5] S. E. Sebastian, N. Harrison, and G. G. Lonzarich, Rep. Prog. Phys. **75**, 102501 (2012).

[6] J. Chang, E. Blackburn, A. T. Holmes, N. B. Christensen, J. Larsen, J. Mesot, R. Liang, D. A. Bonn, W. N. Hardy, A. Watenphul, M. v. Zimmermann, E. M. Forgan, and S. M. Hayden, Nat. Phys. **8**, 871 (2012).

[7] S. Gerber, H. Jang, H. Nojiri, S. Matsuzawa, H. Yasumura, D. A. Bonn, R. Liang, W. N. Hardy, Z. Islam, A. Mehta, S. Song, M. Sikorski, D. Stefanescu, Y. Feng, S. A. Kivelson, T. P. Devereaux, Z.-X. Shen, C.-C. Kao, W.-S. Lee, D. Zhu, and J.-S. Lee, Science **350**, 949 (2015).

[8] A. A. Yurgens, Supercond. Sci. Technol. **13**, R85 (2000).

[9] E. L. Wolf, *Principles of Electron Tunnelling Spectroscopy* (Oxford University Press, New York, 1989), Chap. 4.

[10] O. Ahmadi, L. Coffey, J. F. Zasadzinski, N. Miyakawa, and L. Ozyuzer, Phys. Rev. Lett. **106**, 167005 (2011).

[11] D. Mandrus, L. Forró, D. Koller, and L. Mihály, Nature (London) **351**, 460 (1991).

[12] D. Mandrus, J. Hartge, C. Kendziora, L. Mihály, and L. Forró, Europhys. Lett. **22**, 199 (1993).

[13] J. R. Cooper, Phys. Rev. B **76**, 064509 (2007).

[14] X.-H. Sui, H. Tang, S. P. Zhao, and Z.-B. Su, Physica C **511**, 15 (2015).

[15] J. P. Carbotte, T. Timusk, and J. Hwang, Rep. Prog. Phys. **74**, 066501 (2011).

[16] T. M. Benseman, J. R. Cooper, and G. Balakrishnan, arXiv:1501.00335.

[17] S. Blanco-Canosa, A. Frano, T. Loew, Y. Lu, J. Porras, G. Ghiringhelli, M. Minola, C. Mazzoli, L. Braicovich, E. Schierle, E. Weschke, M. Le Tacon, and B. Keimer, Phys. Rev. Lett. **110**, 187001 (2013).

[18] Th. Jacobs, S. O. Katterwe, and V. M. Krasnov, Phys. Rev. B **94**, 220501(R) (2016).

[19] J. W. Loram, J. Luo, J. R. Cooper, W. Y. Liang, and J. L. Tallon, J. Phys. Chem. Solids **62**, 59 (2001).

[20] T. Watanabe, T. Fujii, and A. Matsuda, Phys. Rev. Lett. **84**, 5848 (2000).

[21] J. L. Tallon, J. W. Loram, J. R. Cooper, C. Panagopoulos, and C. Bernhard, Phys. Rev. B **68**, 180501(R) (2003).

[22] W. Anukool, S. Barakat, C. Panagopoulos, and J. R. Cooper, Phys. Rev. B **80**, 024516 (2009).

[23] A. Larkin and A. Varlamov, *Theory of Fluctuations in Superconductors* (Clarendon Press, Oxford, UK, 2005).

[24] M. R. Presland, J. L. Tallon, R. G. Buckley, R. S. Liu, and N. E. Flower, Physica C **176**, 95 (1991).

[25] H. Won and K. Maki, Phys. Rev. B **49**, 1397 (1994).

[26] T. M. Benseman, Ph.D thesis, University of Cambridge, 2007.

[27] X. B. Zhu, Y. F. Wei, S. P. Zhao, G. H. Chen, H. F. Yang, A. Z. Jin, and C. Z. Gu, Phys. Rev. B **73**, 224501 (2006).

[28] V. M. Krasnov, A. Yurgens, D. Winkler, P. Delsing, and T. Claeson, Phys. Rev. Lett. **84**, 5860 (2000).

[29] R. C. Dynes, V. Narayanamurti, and J. P. Garno, Phys. Rev. Lett. **41**, 1509 (1978).

[30] M. Eschrig, Adv. Phys. **55**, 47 (2006).

[31] In the simple picture used here, $\mathbf{k}$ cannot be conserved exactly because an electron in the final state in electrode 2 has a higher

energy relative to the bottom of the band than in the initial state in electrode 1, and therefore must have a larger value of $|\mathbf{k}|$, but this is a relatively small effect of order eV/E_F where e is the charge of an electron and E_F is the Fermi energy measured from the bottom of the band.

[32] O. K. Andersen, A. I. Liechtenstein, O. Jepsen, and E. Paulsen, J. Phys. Chem. Solids **56**, 1573 (1995).

[33] J. W. Loram (personal communication).

[34] Yu. I. Latyshev, T. Yamashita, L. N. Bulaevskii, M. J. Graf, A. V. Balatsky, and M. P. Maley, Phys. Rev. Lett. **82**, 5345 (1999).

[35] N. Morozov, L. N. Bulaevskii, M. P. Maley, Yu. I. Latyshev, and T. Yamashita, Phys. Rev. B **62**, R14681 (2000).

[36] I. Vekhter, L. N. Bulaevskii, A. E. Koshelev, and M. P. Maley, Phys. Rev. Lett. **84**, 1296 (2000).

[37] M. Tinkham, *Introduction to Superconductivity*, 2nd ed. (McGraw-Hill, Inc., New York, 1996), Chap. 10.

[38] We normalize by dividing through by polynomials $(a + bV^2 + cV^4) \times 10^{-3}\ \Omega^{-1}\ \mu\mathrm{m}^{-2}$. The constants a, b, and c were found by requiring normalized dI/dV curves for $H = 13$ T and 1.4 K, to be unity at high V, 0.142–0.15 V, with zero slope and to conserve states between 0 and 0.15 V to within 1% or better. The values of the coefficients are $a = 13.0$, 8.85, and 5.305, $b = -380.6$, -151.27, and -138.75, $c = 3113$, 501.22, and 1670, for mesas OD78, OD80, and OP86, respectively. This procedure was used for the data in Figs. 2(b), 5(b), 5(c), 7, 8(a), and 12(b). The data for OD80 in Figs. 8(b)–8(f) are normalized by applying the same procedure to the dI/dV curve for $H = 0$ T and 1.4 K, giving values of $a = 9.25$, $b = -227.6$, and $c = 3025.6$. In Fig. 13, "norm1" and "norm2" refer to the 13 T and 0 T normalizing polynomials, respectively. Choice of the correct background will be important for Eliashberg analysis of the dip in dI/dV near 0.13 V shown in Fig. 5(c).

[39] A. Junod, K.-Q. Wang, T. Tsukamoto, G. Triscone, B. Revaz, E. Walker, and J. Muller, Physica C **229**, 209 (1994).

[40] S. Ozcan, P. J. Turner, J. R. Waldram, R. J. Drost, P. H. Kes, and D. M. Broun, Phys. Rev. B **73**, 064506 (2006).

[41] Y. Wang, B. Revaz, A. Erb, and A. Junod, Phys. Rev. B **63**, 094508 (2001).

[42] S. C. Riggs, O. Vafek, J. B. Kemper, J. B. Betts, A. Migliori, F. F. Balakirev, W. N. Hardy, R. X. Liang, D. A. Bonn, and G. S. Boebinger, Nat. Phys. **7**, 332 (2011).

[43] C. Marcenat, A. Demuer, K. Beauvois, B. Michon, A. Grockowiak, R. Liang, W. Hardy, D. A. Bonn, and T. Klein, Nat. Commun. **6**, 7927 (2015).

[44] See Supplemental Material at http://link.aps.org/supplemental/10.1103/PhysRevB.98.014507 for raw data for the three mesas in Fig. 1 and $I(V)$ and dI/dV data for OD80 in Figs. 5, 6, and 12(a).

[45] L. Forró, Phys. Lett. A **179**, 140 (1993).

[46] G. Soda, D. Jérome, M. Weger, J. Alizon, J. Gallice, H. Robert, J. M. Fabre, and L. Giral, J. Phys. France **38**, 931 (1977).

[47] J. R. Cooper and B. Korin-Hamzić, in *Organic Conductors*, edited by J.-P. Farges (M. Dekker Inc., New York, 1994), p. 377.

[48] G. E. Volovik, JETP Lett. **58**, 469 (1993).

[49] A. F. Bangura, P. M. C. Rourke, T. M. Benseman, M. Matusiak, J. R. Cooper, N. E. Hussey, and A. Carrington, Phys. Rev. B **82**, 140501R (2010).

[50] H. He, Y. Sidis, P. Bourges, G. D. Gu, A. Ivanov, N. Koshizuka, B. Liang, C. T. Lin, L. P. Regnault, E. Schoenherr, and B. Keimer, Phys. Rev. Lett. **86**, 1610 (2001).

[51] D. J. Scalapino, Rev. Mod. Phys. **84**, 1383 (2012).

[52] G. Mihály, A. Halbritter, L. Mihály, and L. Forró, Solid State Commun. **116**, 197 (2000).

[53] J. Bruér, I. Maggio-Aprile, N. Jenkins, Z. Ristić, A. Erb, C. Berthod, Ø. Fischer, and C. Renner, Nat. Commun. **7**, 11139 (2016).

[54] M. Suzuki, T. Watanabe, and A. Matsuda, Phys. Rev. Lett. **82**, 5361 (1999).

[55] J. L. Tallon, F. Barber, J. G. Storey, and J. W. Loram, Phys. Rev. B **83**, 092502 (2011).

[56] T. Kondo, W. Malaeb, Y. Ishida, T. Sasagawa, H. Sakamoto, T. Takeuchi, T. Tohyama, and S. Shin, Nat. Commun. **6**, 7699 (2015).

[57] T. J. Reber, S. Parham, N. C. Plumb, Y. Cao, H. Li, Z. Sun, Q. Wang, H. Iwasawa, M. Arita, J. S. Wen, Z. J. Xu, G. D. Gu, Y. Yoshida, H. Eisaki, G. B. Arnold, and D. S. Dessau, arXiv:1508.06252.

[58] J. G. Storey, New J. Phys. **19**, 073026 (2017).

[59] Y. Koval, F. Chowdhury, X. Jin, Y. Simsek, F. Lichtenberg, R. Pentcheva, and P. Müller, Phys. Status Solidi A **208**, 284 (2011).

[60] I. Kokanović, D. J. Hills, M. L. Sutherland, R. Liang, and J. R. Cooper, Phys. Rev. B **88**, 060505(R) (2013).